# Compositional Analysis of an Impact Polypropylene Copolymer by Fast Scanning DSC and FTIR of TREF–SEC Cross-Fractions

**DATASET** · JULY 2012



**5 AUTHORS**, INCLUDING:

Vincent B. F. Mathot
University of Leuven
**111** PUBLICATIONS **2,262** CITATIONS

Macromolecules

Article

pubs.acs.org/Macromolecules

# Compositional Analysis of an Impact Polypropylene Copolymer by Fast Scanning DSC and FTIR of TREF-SEC Cross-Fractions

Sadiqali Cheruthazhekatt,[†] Thijs F. J. Pijpers,[‡,§] Gareth W. Harding,[†] Vincent B. F. Mathot,[‡,§] and Harald Pasch*[,†]

[†]Department of Chemistry and Polymer Science, University of Stellenbosch, 7602 Matieland, South Africa

[‡]SciTe, Ridder Vosstraat 6, 6162 AX Geleen, The Netherlands

[§]Polymer Chemistry and Materials, Department of Chemistry, Katholieke Universiteit Leuven, Celestijnenlaan 200F, 3001 Heverlee, Belgium

**ABSTRACT:** For the first time, the complex composition of a two-reactor-produced impact polypropylene copolymer (IPC) has been fully revealed by advanced thermal analysis, using the combination of fast scanning DSC (HPer DSC, flash DSC, and solution DSC) with SEC fractionation subsequent to TREF fractionation. The dual TREF-SEC separation provided fractions of a few micro- or nanograms that were used to correlate the molecular structure of the polymer chains and their thermal properties (melting and crystallization behavior of the different macromolecules under a variety of different conditions). The SEC fractions were collected using the LC transform interface and subjected to FTIR and fast scanning DSC analysis. The SEC curves showed mono-, bi-, and multimodal molar mass distributions. The SEC fractions collected were analyzed by HPer DSC at 50 °C/min by which the thermal properties of the fractions could be established and salient details revealed. The findings were confirmed by structural information that was obtained using FTIR measurements. These results confirmed that even after TREF fractions were obtained they were complex regarding molar mass and chemical composition. By applying HPer DSC at scan rates of 5−200 °C/min and flash DSC at scan rates of 10−1000 °C/s, the metastability of one of the fractions was studied in detail. The high molar mass part of the material appeared to be constituted of both highly isotactic PP and low to medium propylene content ethylene copolymers (EPC). The medium molar mass part consisted of high to medium isotactic PP and of low propylene content EPC. The low molar mass part did not show ethylene crystallinity; only propylene crystallinity of medium to low isotacticity was found. DSC measurements of TREF-SEC cross-fractions at high scan rates in *p*-xylene successfully connected reversely to the slow scan rate in TREF elution, if corrected for recrystallization. All EPC's show only ethylene-type crystallization. The wealth of information obtainable from these method combinations promises to be extremely useful for a better understanding of the melting and crystallization processes of such complex materials. The ability to run DSC experiments at very high scan rates is an important prerequisite to understanding the melting and crystallization behavior under conditions that are very close to melt processing of these key commodity polymers.

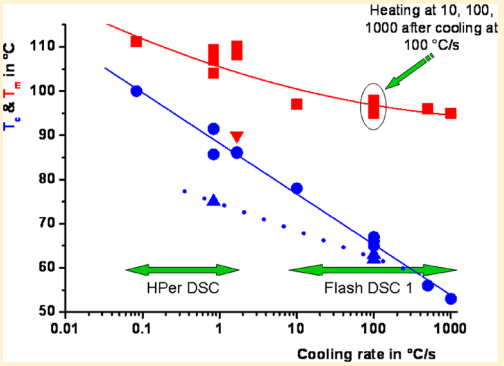


## 1. INTRODUCTION

Although polyolefins have existed for a long time, some of the various types of polyethylenes and polypropylenes still pose quite a challenge to reveal their detailed molecular structure in order to understand its relations with the catalyst and polymerization conditions applied on one hand and with the properties as modulated by processing on the other.[1] For some types the link between the two is pretty straightforward, meaning that mainly the chain structure defines the properties. This is the case for ethylene-based rubbers where the sequence length distribution of the crystallizable ethylene units is the main variable. However, this is an exception. Normally, appreciable variations are possible if one can change the topology of the chains and the way of crystallization considerably. Examples are the applications of UHMWPE for producing both strong fibers by way of extending most of the chains, and fixation of that topology by crystallization, as well as its use for linears of skis, by way of forming a low-crystalline coating leading to decreasing resistivity. Crystallization also culminates in a final morphology with consequences for optical behavior, permeability, etc. The crystallization capability strongly depends on the molecular structure or chain architecture on one hand and the way of handling/processing on the other.

Therefore, it is crucial to investigate these phenomena and to explore their possible interactions by performing a detailed analysis of the molecular structure and linking it to the crystallization behavior under the (process) conditions of interest. Recently, some very interesting, new characterization tools became available, which are discussed in this report. First

**Received:** April 30, 2012
**Revised:** July 4, 2012
**Published:** July 19, 2012

   dx.doi.org/10.1021/ma3008702 | *Macromolecules* 2012, 45, 5866−5880

of interest for determining the detailed molecular structure, high-temperature HPLC with cross-fractionation by SEC (HT-2D-LC) has become available for the analysis of IPC's.[2] Second, for exploration of the capabilities of a specific polyolefin to crystallize, the recently introduced fast scanning calorimeters (FSC[3−5]), high performance DSC (HPer DSC[6]), and flash DSC 1[7] are great tools.

To investigate to what extent these tools can be of use, ongoing research on IPC is taking place.[2,8] It is known for a long time that IPC is a complex polymer system, being a blend of various types of polyolefins: ethylene−propylene rubber (EPR), various propylene-copolymerized polyethylenes (ethylene−propylene copolymers, EPC), and polypropylene (PP) chains having a variety of tacticities. The majority of the chains are isotactic in nature, which in practice means that other, minor components can be partly overshadowed or even overruled when these IPC's are characterized in bulk, even though from a properties' point of view these minor components can be crucial. The cause of this complex molecular structure is found in the choices made in combining a heterogeneous Ziegler−Natta catalyst and the method of polymerization. The present PP studied has been polymerized in a two-reactor setup.

From the very early days of polyolefins onward, many research groups have aimed at solving the problem of determination of the complex structure of impact PP by trying to separate its constituents physically.[9,10] A number of (cross) fractionation methods have been applied with variable success. A popular method of fractionation is temperature rising elution fractionation (TREF) (see ref 11 for early references). The technique makes use of the differences in crystallizability of the various components, especially as a function of temperature. The cooling rate is set very low, typically 1 °C/h, decreasing from a high temperature (e.g., 130 °C) in a solvent (e.g., xylene) and at a concentration of ∼1 wt %. By using such a slow rate, it is expected to separate the components present as completely as possible by selective crystallization and to avoid reorganization effects during dissolution by heating in the next step. Co-crystallization should also be minimized, as the (segments of) chains are expected to have ample time to crystallize by searching for equals or on their own. During the stepwise, faster heating (typically at 0.5 °C/min) of the elution step, it is assumed that chains dissolve without too much reorganization and that they are removed from the solution at increasing temperatures. The amount of removed polymer material is subsequently determined, and the fractions are possibly studied further with regards to composition and molar mass.

A few remarks can be made regarding TREF fractionation. First, at a concentration of 1 wt % the macromolecules experience a situation between a dilute solution and a melt according to Mandelkern;[12] therefore, molar mass comes into play because the chains are still entangled causing crystallization to be hindered.[11] Second, even during such slow cooling and subsequent heating, reorganization can take place.[13] It is of importance to realize that the chains dissolve only when the most stable segment of the chain dissolves, which is usually related to the longest sequence of a crystallizable unit in the case of a branched polymer or copolymer. Thus, the earlier dissolution of less stable sequences goes unnoticed. The so-called "amorphous" fraction, which relates to amorphous behavior at room temperature, could have crystallizability at subambient temperatures down to the glass transition, significantly altering mechanical properties at subambient temperatures.

A major problem is that two apparently different components can still elute at the same TREF temperature. This possibility arises because—from the temperature point of view—such components could be different with respect to their temperature ranges of crystallization and melting in case one works without solvent, directly from the melt. Using a solvent in TREF or in crystallization analysis fractionation (CRYSTAF[14]), fractionations can nevertheless bring such ranges closer to each other or move them farther from each other, depending on constitution and interaction.

Actually, bringing the crystallization ranges closer to each other can be the case for PP blends containing ethylene-based components. Although these components could have dissimilar crystallizing and melting temperature ranges from polypropylene in the melt, in solution they can end up in similar temperature ranges because the depressions of these ranges by the solvent can be different for the respective components; e.g., they can be substantially larger for PP than for ethylene-based components. Of course, in such a case the separation of the components is difficult to realize. Still, the possibility remains to perform a second (cross) fractionation with another technique, e.g., SEC. Indeed, TREF-SEC has been applied for ethylene−1-pentene copolymers[15] and bimodal HDPE,[16] and the use of this method will also be the subject of this paper.

It should be pointed out that fractionation and evaluation of the results would be more straightforward if the cross-fractionation was done in the reverse order, e.g., SEC or direct extraction (DE)[17,18] followed by TREF,[11,19] because SEC is only slightly influenced by comonomer content or short chain branching; therefore, the first fractionation step according to molar mass would be almost unequivocal, while the second step, TREF, acts on chain composition by way of crystallization of the molar mass fractions obtained by SEC.

New, exciting possibilities lie ahead, especially by application of HT-2D-LC. HT-2D-LC separates according to chemical composition, but not via a crystallization route as in TREF and CRYSTAF.[20−23] SEC can then be applied as the second step in this cross-fractionation. The first results have been published[2] and show a crystallization-independent fractionation with good resolution toward the various components present.

In all cases, be it combinations of TREF, HT-SEC, or HT-HPLC, it is necessary to add other characterization techniques for complete unraveling of the molecular structure. Among the techniques capable to work on the (often) minute amounts of (cross) fractions, FTIR and DSC turn out to be very useful. Besides providing additional information regarding the chemical constitution, FTIR also detects molecules that are in the (semi)crystalline state. DSC measures the thermal properties and information about crystallizability is obtained. The combination of these techniques provides a powerful set of tools for in-depth characterization of crystallizable polymers, as is shown in this paper for the combinations of TREF-SEC-LC transform with FTIR and FSC. In this setup, the LC transform interface instrument is used to collect the polymer fractions from the SEC elution on a disk by removing the solvent at high temperature and at the same time cooling and depositing the sample onto the disk. The collected fractions are then directly measured by off-line FTIR and FSC.


dx.doi.org/10.1021/ma3008702 | Macromolecules 2012, 45, 5866−5880

## 2. EXPERIMENTAL SECTION

A nonstabilized IPC, designated as 3V, was obtained from SASOL Polymers (Secunda, South Africa). The IPC sample has a comonomer (ethylene) content of 10.5 mol %, with a weight-average molar mass ($M_w$) and dispersity ($D$) of 228 kg mol$^{-1}$ and 3.5, respectively.

**Size Exclusion Chromatography (SEC).** Molar mass measurements for all samples were performed at 150 °C using a PL GPC 220 high temperature chromatograph (Polymer Laboratories, Church Stretton, U.K.) equipped with a differential refractive index (RI) detector. The column set used consisted of three 300 × 7.5 mm PLgel Olexis columns together with a 50 × 7.5 mm PLgel Olexis guard column (Polymer Laboratories, Church Stretton, U.K.). The eluent used was TCB at a flow rate of 1.0 mL/min with 0.0125% 2,6-di-*tert*-butyl-4-methylphenol (BHT) added as a stabilizer. Samples were dissolved at 160 °C in TCB at a concentration of 1 mg/mL for 1−2 h (depending on the sample type), and 200 μL of each sample was injected. Narrowly distributed polystyrene standards (Polymer Laboratories, Church Stretton, U.K.) were used for calibration.

**Temperature Rising Elution Fractionation (TREF).** Preparative TREF was carried out using an instrument developed and built in-house. Approximately 3.0 g of polymer (concentration of ∼1 wt %) and 2.0% w/w Irganox 1010 (Ciba Specialty Chemicals, Switzerland) were dissolved in 300 mL of xylene at 130 °C in a glass reactor. The reactor was then transferred to a temperature-controlled oil bath and filled with sand (white quartz, Sigma-Aldrich, South Africa), used as a crystallization support. The oil bath and support were both preheated to 130 °C. The oil bath was subsequently cooled to room temperature at a controlled rate of 1 °C/h in order to facilitate the controlled crystallization of the polymer. Next, the crystallized mixture was packed into a stainless steel column which was inserted into a modified gas chromatography oven for the elution step. Preheated xylene was used as eluent in order to collect the fractions in heating at predetermined temperatures ranging from 30 to 130 °C with isothermal stays of 20 min. The fractions were isolated by precipitation in acetone, followed by drying to a constant mass.

**Deposition of SEC Fractions by the LC Transform Interface.** An LC transform series model 303 (Lab Connections) was coupled to the PL GPC 220 in order to collect the SEC eluate. Samples were dissolved at 160 °C in TCB at a concentration of 2 mg/mL with 200 μL (in total 0.4 mg) of each sample being injected. The SEC column outlet was connected to the LC transform interface through a heated transfer line set at 150 °C. The fractions are usually deposited on a germanium disk (sample target in the LC transform) rotating at a speed of 20°/min. The disk stage and nozzle temperatures of the LC transform were set to 160 and 150 °C, respectively. For HPer DSC sample preparation an aluminum foil was wrapped around the germanium disk in such a way as to ensure good contact with the disk, with the opaque side of the foil being used for collection of the polymer deposits. The surface roughness of the opaque side of the foil enables comparatively higher adhesion as compared to the glossy side of the Al foil. The bulk sample was collected by deposition of the entire sample at a single point on the germanium disk (no rotation) in order to give it the same SEC history as the fractions thereof. All samples for SEC-FTIR and SEC-HPer DSC, including the bulk polymer 3V, were prepared under the same deposition and cooling conditions in order to ensure comparable sample and thermal histories. Therefore, the FTIR results—especially the crystallinity results—are based on these cooling conditions and by that, strictly spoken, comparable with results obtained from the first heating curve of the DSC used. Mostly, the first and second heating curves reported here are not very different, though sometimes the area and/or the position of the melting peak maximum is different (see e.g. Figure 10a).

**FTIR Analyses of the Deposited Fractions.** FTIR analyses of the deposited SEC fractions were performed on a Thermo Nicolet iS10 spectrometer (Thermo Scientific, Waltham, MA), equipped with the LC transform FTIR interface connected to a standard transmission base plate. Spectra were recorded at a resolution of 8 cm$^{-1}$ with 16 scans being recorded for each spectrum. Thermo Scientific OMNIC software (version 8.1) was used for data collection and processing.

**Fast Scanning Calorimetry by HPer DSC and Flash DSC 1.** Thermal properties of the TREF-SEC-LC transform interface deposits were investigated using two types of power-compensating, twin-type FSC's: a Perkin-Elmer DSC 8500 with an intracooler at −120 °C and a MEMS-technology, chip-based calorimeter flash DSC 1 of Mettler-Toledo,[6] both situated at SciTe's laboratory, Katholieke Universiteit Leuven, Belgium.

A single deposition on the aluminum foil delivers enough material (not weighed as yet) for measurement in both cooling and heating by the DSC 8500 at a standard rate of 50 °C/min between 0 and 200 °C, but usually plotted from 0 or 20 to 180 °C. Because the sample mass was not known, in the calculations and figures a sample mass of 1 mg has been taken. Isothermal stays at the start and end temperatures were 3 min. For measurement, the aluminum foil with the sample deposited is cut between various rotation angles. The sample on the foil is then folded into a flat package for analysis at the sample spot of the DSC 8500. At the reference spot an (empty) aluminum foil is placed. Nitrogen is used as a purge gas. Most curves are corrected by subtracting an empty-cell curve. In addition, all curves have been corrected for thermal lag for the various cooling and heating rates applied. For the measurements in xylene (consisting of 98% *p*-xylene) in between room temperature and 130 °C with an isothermal stay of 15 min at 130 °C, the aluminum foil with the sample was placed in a large volume capsule (LVC) pan with 20 μL of xylene. As the SEC-LC transform interface is loaded with 200 μL containing 0.4 mg, ∼0.04−0.2 mg of sample will be in solution (supposing the sample mass is about 10−50 wt % of the total TREF fraction mass respectively), leading to a concentration of ∼0.2−1 wt %. This is to be compared with the typical TREF concentration of ∼1 wt %.

In the case of the flash DSC 1, part of the sample deposited on the aluminum foil is scraped and put on the sample hotspot of the sensor and measured at a standard rate of 100 °C/s between room temperature and 200 °C but plotted until 160 °C. For both DSCs also other scan rates have been applied: 5, 10, (50), 100, and 200 °C/min for the DSC 8500 and 10, (100), 500, and 1000 °C/s in cooling and heating for the flash DSC 1. First heating, first cooling, and second heating curves have been measured and plotted (endo up, exo down). All transitions observed turned out to be either crystallization (during cooling, curves in blue) or melting (during heating, curves in red) and possibly recrystallization (meaning the sample follows the sequence melting−recrystallization−remelting during heating).

## 3. RESULTS AND DISCUSSION

The elucidation of the molecular structure of the IPC 3V is accomplished by studying thermal properties using DSC, with additional information from FTIR. For detailed information on the IPC and on the fractionation techniques used, the reader is referred to a recent paper.[2] In short, the bulk IPC 3V sample was fractionated by TREF. In total, eight fractions were obtained at 30, 60, 80, 90, 100, 110, 120, and 130 °C elution temperatures, which are coded as 3V *x.y*, with *x* denoting the TREF elution temperature. The number of depositions (on the LC transform disk) prepared is denoted by $y$ = 1, 2, and 3, leading to codes such as 3V 80.2. One deposition delivers enough material for the DSC 8500 to result in DSC curves with reasonable to good heat flow rates. All samples deposited are reported in this report, except for TREF fractions 30, 100, and 120 °C. Because of the fact that the 30 °C TREF fraction is such an important fraction, and also a major constituent of most IPC's, it was decided to investigate the (sub)ambient crystallization in more detail in a subsequent study. A thorough evaluation of the complex composition of the 30 °C TREF fraction is very important, especially with regard to its influence on the low-temperature mechanical properties of the IPC. The two higher temperature fractions (100 and 120 °C) are known

to be mainly isotactic PP, and so there is not much new information that could be expected from these fractions.

Figure 1 shows the resulting mass distribution constituted by the TREF fractions obtained per temperature increment. As can

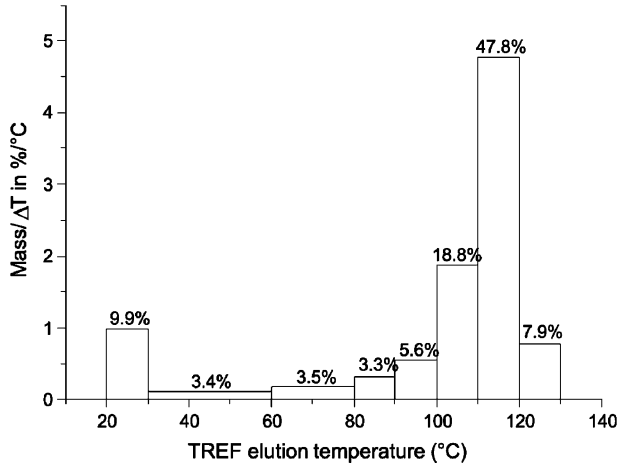


**Figure 1.** Mass distribution in percent per temperature increment as a function of the elution temperature for the TREF fractions obtained.

be seen, an appreciable amount of material elutes already at 30 °C. This amorphous fraction also contains components which are crystallizable at (sub)ambient temperatures. For these components, the often-used wording "amorphous fraction" just describes the situation at 30 °C. It also reflects the fact that it is difficult to perform TREF at (sub)ambient temperatures because solvents such as *p*-xylene will crystallize, and one may face technical problems of operating and handling at lowered temperatures.

In ref 8 the corresponding DSC second heating curves of the TREF fractions of 30−120 °C were reported, as measured from 25 to 200 at 10 °C/min. The authors concluded that no melting endotherm is present in the 30 °C fraction as was expected for a random ethylene−propylene copolymer (EP rubber). All fractions eluting from 60 to 100 °C exhibit two melting endotherms, namely at 89 and 112 °C (fraction 60 °C), 103 and 130 °C (fraction 80 °C), 118 and 146 °C (fraction 90 °C), 118 and 150 °C (fraction 100 °C). Clearly, in melting subsequent to crystallization from the melt, these polymer fractions show such distinct melting temperatures, and the presence of (at least) two crystallizable components melting at different temperatures must be assumed that are caused by appreciable differences in molecular structures.

The 110 and 120 °C fractions show single, distinct melting peaks at 159 and 161 °C, respectively, which are ascribed to highly isotactic PP. With increasing TREF elution temperatures, the peak areas increase indicating increasing crystallinities. Data on the 130 °C fraction were not available: they are expected to be similar to the 100 and 110 °C fractions.

Elution at one and the same TREF temperature, and bimodality of the melting point distribution, as seen for some of the DSC curves, can have various causes. First, crystallization in a solvent under TREF conditions is different from crystallization from the melt for various reasons. The molar mass influence on crystallization is appreciable for the pure polymer, while in solution the influence is dependent on the quality of the solvent and the concentration. Second, for the present case, molecules that dissolve at one and the same TREF elution temperature can also do so because the melting point depression caused by the solvent ($T_m^{melt} - T_m^{solution}$) is larger for a polymer with propylene crystallinity than in the case of ethylene crystallinity. In this way, differences in e.g. maximum or end melting points in the case of melt crystallization between molecules having ethylene-based (PE: various amounts of propylene incorporated in the chains) and propylene-based (PP: various isotacticities) crystallization can be (partly) canceled by having crystallization done in a solvent; see further on at the analysis of the 80 °C (Figure 6b) and 90 °C (Figure 8b) TREF fractions.

In order to determine possible differences in melting behavior across the MMD, each of the TREF fractions was fractionated according to molar mass by HT-SEC; see Figure 2, showing all SEC curves obtained on the (bulk) 3V, and on 3V *x.y* samples.

The SEC curves are plotted in their respective temperature ranges of elution. For example: fraction 3V 100 is plotted in

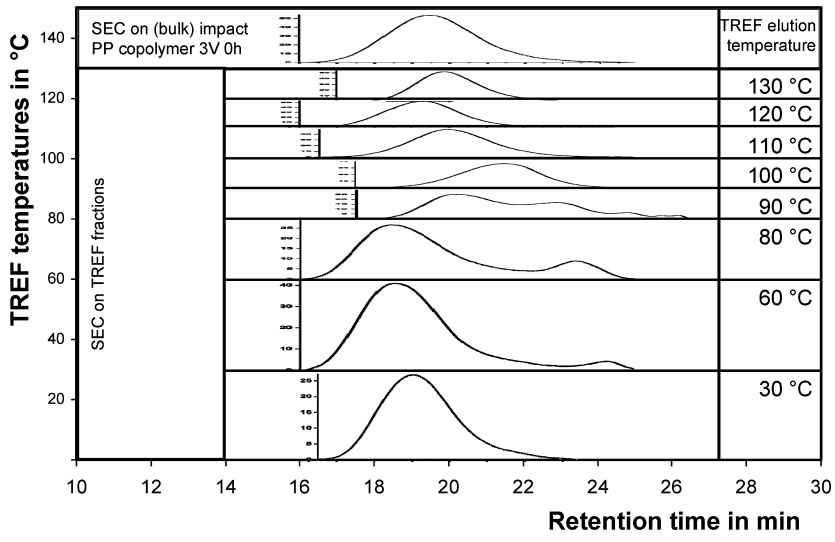


**Figure 2.** High-temperature SEC curves obtained on the (bulk) 3V (top) and on 3V TREF fractions thereof as obtained at various TREF elution temperatures: 30, 60, 80, 90, 100, 110, 120, and 130 °C. See text for explanation.


dx.doi.org/10.1021/ma3008702 | *Macromolecules* 2012, 45, 5866−5880

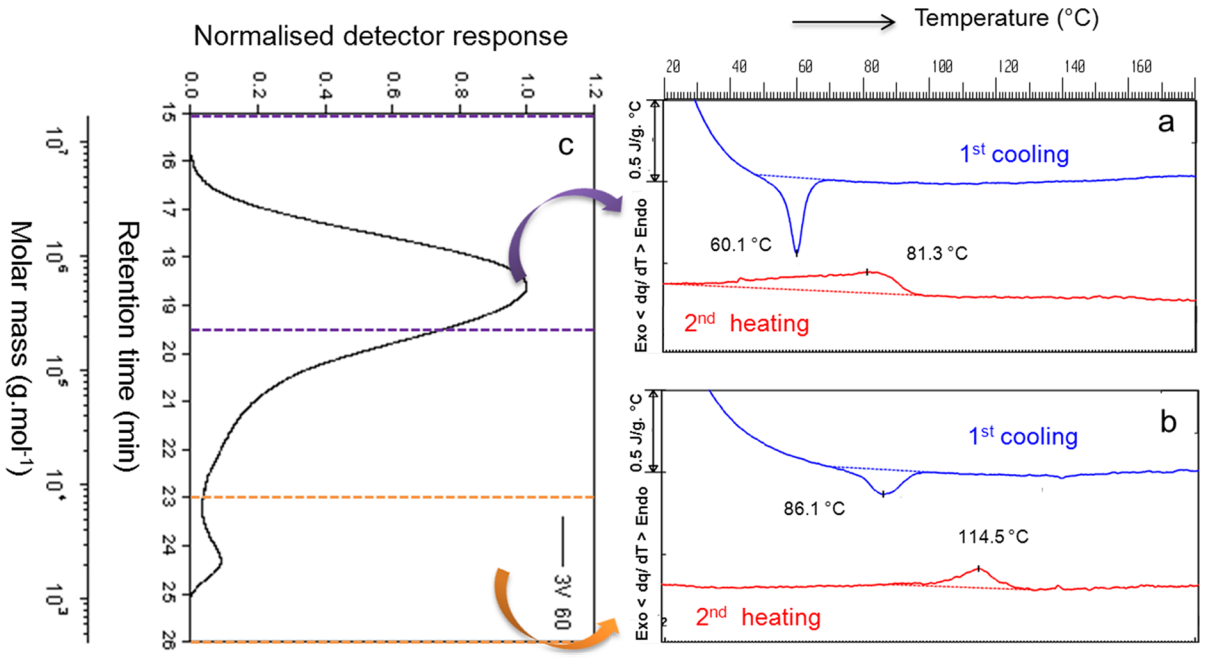


**Figure 3.** SEC-DSC analysis of sample TREF 3V 60. DSC curves of first cooling and second heating of two SEC fractions of TREF fraction 3V 60.

between the temperatures 90 and 100 °C, since it has been obtained by elution in that temperature range; the preceding fraction 3V 90 covered the temperature range from 80 until 90 °C, and the next fraction 3V 110 is plotted in the range from 100 to 110 °C, and so forth.

From this plot it is clear that some fractions are bimodal, meaning that part of the low molar mass polymer chains are dissolved at the same temperature as a part of the high molar mass polymer chains. One may wonder whether the bimodality of the SEC curves, seen for the 60, 80, and 90 °C TREF fractions, is connected with the bimodality of the 60, 80, 90, and 100 °C TREF fractions seen in the DSC curves[8] (see earlier remark). The next part of this topic is addressed on the basis of TREF-SEC cross-fractions, using DSC and FTIR analyses after deposition on a disk by the LC transform interface. Details of the experimental method using the LC transform interface can be found in the Experimental Section and in ref 2.

**Analysis of the Bulk Sample.** In the preceding paper,[2] results on the bulk sample 3V have been discussed in detail. The crystallization and melting behavior by HPer DSC at 10 and 50 °C/min was seen to be dominated by the high-isotacticity PP molecules present, overshadowing the other components in the PP system. The FTIR information regarding the PP and PE content and the PP and PE crystallinities confirm this conclusion: the propylene content across the MMD is constant, and the ethylene content of 10.5 mol % is essentially zero, as the level is too low to be detected (in the bulk sample), across the MMD. Similarly, the propylene crystallinity showed to be constant. However, no ethylene crystallinity is noticed; most probably its contribution is too low to be detected, as it is overshadowed by the PP. The crystallization behavior is sensitive to the cooling rate: changing from 10 to 50 °C/min lowers the crystallization peak maximum temperature by 10 °C. However, in both cases the subsequent heating at 50 °C/min leads to a melting peak maximum temperature of 159 °C. Therefore, it is quite obvious that reorganization takes place during heating and is not hindered by the heating rate of 50 °C/min.

**Analysis of TREF Fraction 3V 60 (3.4 wt % of Total).** This is the first TREF fraction with a bimodal MMD (see Figure 3c) and with two melting peaks in the DSC curve (see ref 8) similar to all DSC curves of TREF fractions up to 100 °C. Two SEC fractions with an extreme difference in molar mass were chosen see Figure 3c): one centered around a molar mass of 1 000 000 g/mol (top box) and the other around 2000 g/mol (bottom box).

These fractions represent the two peaks in the SEC curve; the corresponding DSC curves reflect the crystallization and melting behavior. The first heating curves resemble those of the second heating and are not plotted here. The DSC curve of the high molar mass part of the MMD suggests to represent an EP copolymer crystallizing around 60 °C and showing a characteristic,[19] broad melting curve with a peak maximum temperature of ~80 °C and an end melting temperature of 95 °C. The curves resemble EP copolymers such as those in ref 24; see e.g. the EP copolymer EJ 207 as a very typical example. This copolymer is slightly random[25−27] and has 10.6 mol % of propylene and $M_n$, $M_w$, $M_z$ of 39 000, 120 000, 220 000 g/mol, respectively. The chain statistics of this EP copolymer is between alternating and random, with a product of copolymer reactivity ratios, $r_E \cdot r_P$ (E: ethylene; P: propylene) of about 0.50. As the statistics of the present TREF fraction is unknown, it is too speculative to make any further conclusions, the more so because the literature example has been polymerized in a very much designed and ideal way, using a single site, vanadium-type catalyst, leading to a homogeneous type of copolymer.[26] For such a copolymer, the melting curve is expected to resemble the broad ethylene sequence length distribution (ESLD), resulting from the copolymerization statistics.[25] The amount of propylene of the whole fraction 3V 60 is much higher—45 mol %[7]—by which most of the propylene units must be located in molecules of the rest of the distribution, and thus is to be found as a propylene-rich part of the MMD in the medium and lower molar mass regions.


dx.doi.org/10.1021/ma3008702 | Macromolecules 2012, 45, 5866−5880

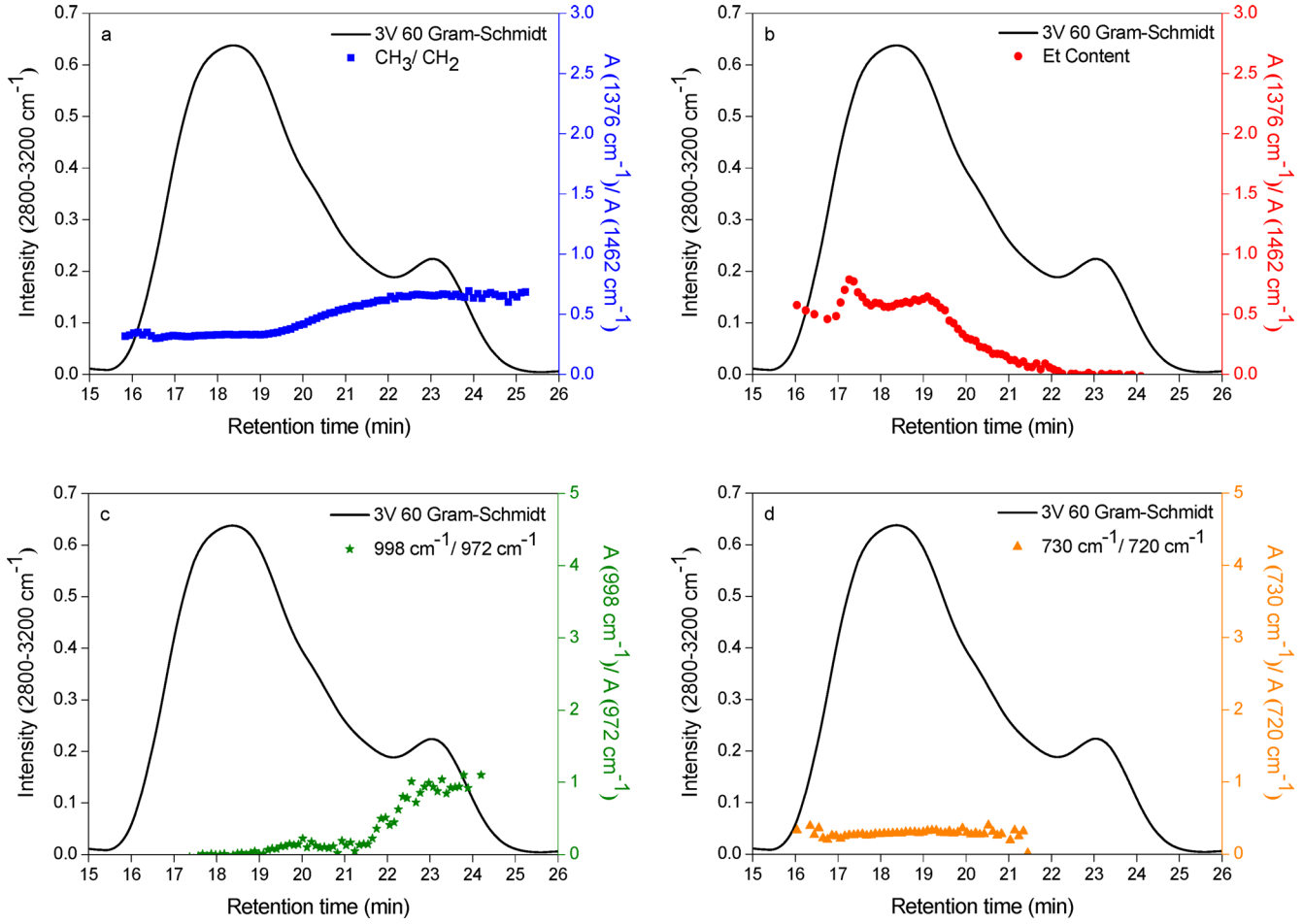


**Figure 4.** SEC-FTIR analysis of the 60 °C TREF fraction (3V 60) illustrating (a) the propylene ($CH_3/CH_2$) and (b) the ethylene (Et content) distributions as well as their crystallinity distributions (c) and (d), respectively.

The DSC curve of the low molar mass part of the MMD suggests to be originating from low-isotacticity PP because the difference, $\Delta T$, between the melting peak maximum temperature of approximately $T_m$ = 115 °C and the crystallization peak maximum temperature of approximately $T_c$ = 86 °C seems to be somewhat too large ($\Delta T = T_m - T_c$ = 30 °C) to be caused by a polyethylene type of crystallization. The occurrence of polypropylene in the lower molar mass region would also account for the rest of the propylene content as mentioned before. The reasoning given is completely confirmed by the FTIR information on the fraction studied (see Figure 4). The composition (propylene and ethylene content) and their crystallinity distributions across MMD are determined as explained in our previous publications.[2,8]

In Figure 4, it is seen that propylene (Figure 4a) is present at all molar masses, and its content increases toward low molar masses. The high molar mass region shows almost exclusively ethylene crystallinity (Figure 4d), while the propylene present is slightly or not crystalline (Figure 4c). In the low molar mass region ethylene is absent (top right) which is why no ethylene crystallinity is noticed (Figure 4d), but only propylene crystallinity (Figure 4c). Both DSC and FTIR results point to a simple explanation of the double melting behavior of the whole TREF fraction 3V 60, as seen in ref 8 and discussed earlier with crystallization/melting peak maximum temperatures of 63 °C/89 °C and 112 °C (at 10 °C/min), namely to connect these to the melting of crystalline structures constituted by ethylene units and propylene units, respectively.

**Analysis of TREF Fraction 3V 80 (3.5 wt % of Total).** In our preceding paper[2] results on TREF fraction 80 °C and SEC fractions thereof have been discussed. Now, extended measurements show additional, interesting information on this sample.

In Figure 5, the MMD of sample TREF 3V 80 is shown as well as crystallization and melting peak maximum temperatures (from second heating) for SEC fractions obtained by DSC. In this figure, three different melting behaviors are seen, and Figure 6 shows characteristic DSC curves, representative for the three groups of samples, distinguishable by their melting behavior:

*Group 1.* Fractions of the middle molar mass part of the MMD, having low melting peak maximum temperatures between 103 and 111 at 50 °C/min cooling/heating rate. In ref 8, 103 °C has been found for the corresponding melting peak at 10 °C/min cooling/heating rate, which makes sense. As an example, in Figure 6a DSC curves are shown of the characteristic sample at 150°−180° (angle on the Ge disk corresponding to a retention time of 20.5−22 min), covering the molar masses as indicated by the red box in Figure 5 (roughly 10−80 kg/mol).

Varying the scan rates from 5, 50, to 100 °C/min, the DSC curves of this sample do not vary much, and values of approximately $T_c \sim 91$ °C and $T_m \sim 110$ °C are found.


dx.doi.org/10.1021/ma3008702 | *Macromolecules* 2012, 45, 5866−5880

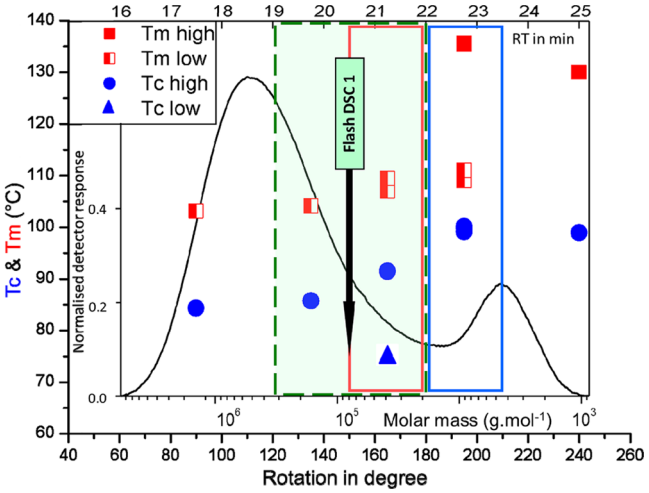


**Figure 5.** SEC separation of sample TREF 3V 80. SEC curve with boxes indicating the molar mass ranges covered by the HPer and Flash DSC measurements shown in Figures 6 and 7 (see text). Red box: middle molar mass part; blue box: low molar mass part; black arrow: molar mass of sample measured by flash DSC 1; green box: molar mass range measured by HPer DSC and combined with flash DSC 1 results (see Figure 7).

*Group 2.* Fractions of the low-*M* part of the MMD have high melting peak maximum temperatures, between 130 and 136 °C, at 50 °C/min cooling/heating rate. For comparison, in ref 8 130 °C has been found for the corresponding melting peak at 10 °C/min cooling/heating rate, which again makes sense. As an example, in Figure 6c, DSC curves are shown of the characteristic sample from 210° to 270° (retention time 23.5–26.5 min), covering the molar masses less than 4000 g/mol.

*Group 3.* As indicated by the blue box in Figure 5, the SEC fraction at 180°–210° (retention time 22–23.5 min) combines the characteristics of groups 1 and 2 by showing both low and high melting temperatures in one and the same curve. Varying the scan rates from 5, 50, 100 to 200 °C/min for this sample results in DSC figures with approximately $T_c \sim 100$ °C and $T_m \sim 136$ °C. In addition, 5 out of 9 measurements done show an additional low-melting peak at ~111 °C in the second heating curve (see the peak at 109 °C in Figure 6b). This suggests that an additional component—and probably a low propylene content EPC—is present of which the melting (peak maximum at 109 °C) is separated from the main medium-isotacticity PP peak (with a maximum at 135.5 °C), while their crystallization peaks coincide at 99.1 °C. It is possible that the nucleation of one of these is triggered by the other.

At least two explanations of this split into three different groups are possible:

First, for PE it has been reported[11] that the melting peak maximum temperature increases when the molar mass is increased from paraffins to high molar mass linear polyethylenes (LPE) in excess of 1 000 000 g/mol. At the same time, the crystallization peak maximum temperature, $T_c$, after an initial increase with increasing $M$ to ~20 000 g/mol, shows a slight decrease up to 60 000 g/mol, after which $T_c$ stays constant until the highest $M$. The explanation is that initially the chain topology in the crystallites changes from extended into folded and that subsequently entanglements set in which hinder crystallization. At >60 000 g/mol $M$ does not affect the crystallization behavior anymore because segments of the long or very long chains crystallize themselves and increasingly independently from the others. Thus, if a chain does not re-enter the same crystallite, either it will stay in the amorphous part or it will crystallize in another crystallite, thereby bridging two crystallites and becoming a tie molecule. The melting behavior does not mimic this behavior because of the occurrence of extensive reorganization by sliding diffusion of chains during cooling after crystallization and subsequent heating toward melting. This specific crystallization behavior is

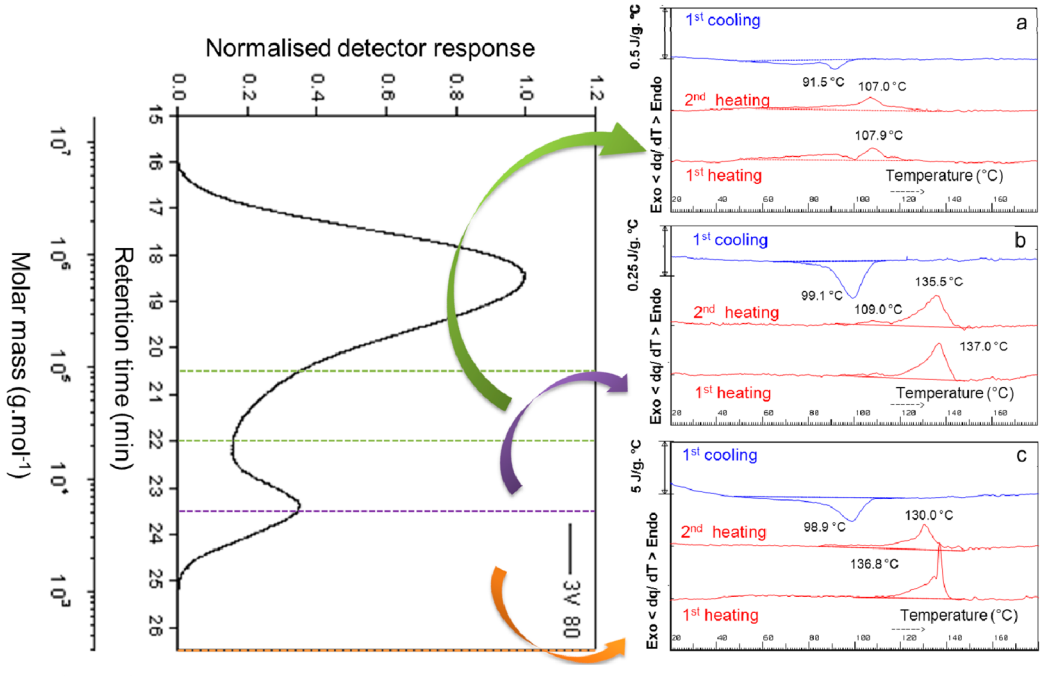


**Figure 6.** DSC analysis of different molar mass fractions of sample TREF 3V 80: (a) a middle-*M* part, see red box in Figure 5; (b) a low-*M* part, see blue box in Figure 5; (c) the lowest-part *M* of less than 4000 g/mol.


dx.doi.org/10.1021/ma3008702 | *Macromolecules* 2012, 45, 5866–5880

strongly dependent on the cooling rate: at lower scan rates the decrease in $T_c$ with increasing $M$ is less; at higher rates $T_c$ decreases appreciably with increasing $M$. For branched polyethylenes, be it either copolymers or branched material like LDPE, the effects have been seen to be stronger, and even the melting behavior becomes affected. For instance LDPE, at constant branching, shows a 12 °C lowering of $T_c$ and 7 °C for $T_m$, occurring at the same apparent molar mass as for LPE. Obviously, reorganization is not possible anymore because the short side chain branching hinders sliding diffusion and by that the process of reorganization is slowed down drastically. One may speculate that PP is affected in the same way, noticing that the abrupt change in $T_m$ by 25−30 °C in Figure 5 also occurs at ∼20 000 g/mol. However, $T_c$ also shows a decrease with increasing $M$ but—in sharp contrast with the PE case—to a lesser extent of about 15 °C and not in an abrupt way.

Second, as before for 3V 60, the differences in $T_m$ and $T_c$ could reflect different molecular structures. The highest molar mass SEC fractions have reasonably narrow crystallization peaks with a long low-temperature tail and broad melting endotherms (see Figure 11 in ref 2), characteristic of polymers with crystallizable ethylene sequence lengths found e.g. in ethylene−propylene copolymers. The low molar mass fractions show much higher melting temperatures, and from the difference between the peak maximum temperatures for melting ($T_m$) and crystallization ($T_c$), $\Delta T = T_m - T_c$, it is supposed that these temperatures point to medium-isotacticity PP.

Evaluating the results obtained with FTIR leads to the conclusion that these confirm the second possibility. This does not necessarily rule out the first one: possibly the melting and crystallization temperature distributions are also lowered partly because of increasing molar mass. It is clear that the bimodal melting behavior reported earlier[8] is explained by the occurrence of the 2 groups of molecules differing in melting behavior, while "intermediate" molecules indicated as group 3 can also show up in the same molar mass range of limited width. It has to be realized that though the melting behavior after crystallization from the melt is very different, all three groups match by eluting in the same TREF temperature range. Interestingly group 3 consists of molecules having the same $M$, meaning that the matching toward the same elution temperature is mainly governed by the ethylene sequences in the ESLD of the low propylene content EPC and governed by the isotactic sequences for the medium-isotacticity PP.

To probe the (meta)stability[28,29] of the crystallites and the occurrence of possible reorganization phenomena, a more extensive evaluation has been performed by applying a variety of combinations of scan rates of 5, 50, 100, and 200 °C/min using HPer DSC. Increasing the cooling rate from the standard rate of 50 to 100 °C/min results in the lowering of the crystallization peak maximum temperature by a maximum of 5 °C. In the case of decreasing the cooling rate to 5 °C/min, crystallization occurs 10 °C higher than at a cooling rate of 50 °C/min. The spread in melting peak maximum temperatures for these cooling conditions is 4 °C at most, which is a rather low value.

Therefore, in addition, the range of scan rates applied was extended appreciably by using the flash DSC 1. For flash DSC, a sample representative of the high molar mass samples was taken at a retention time of 20.5 min by scraping it off the disk. This retention time corresponds to a rotation angle of 150° and an approximate molar mass of 80 000 g/mol, as is seen in Figure 5, black arrow. For linking the data of flash DSC 1 and HPer DSC, samples around this retention time were involved by including measurements by HPer DSC on retention times of 19−20.5 and 20.5−22 min, represented in Figure 5 by the green box.

Figure 7a shows the flash DSC 1 first cooling and second heating curves for the sample at 20.5 min. In Figure 7b, the

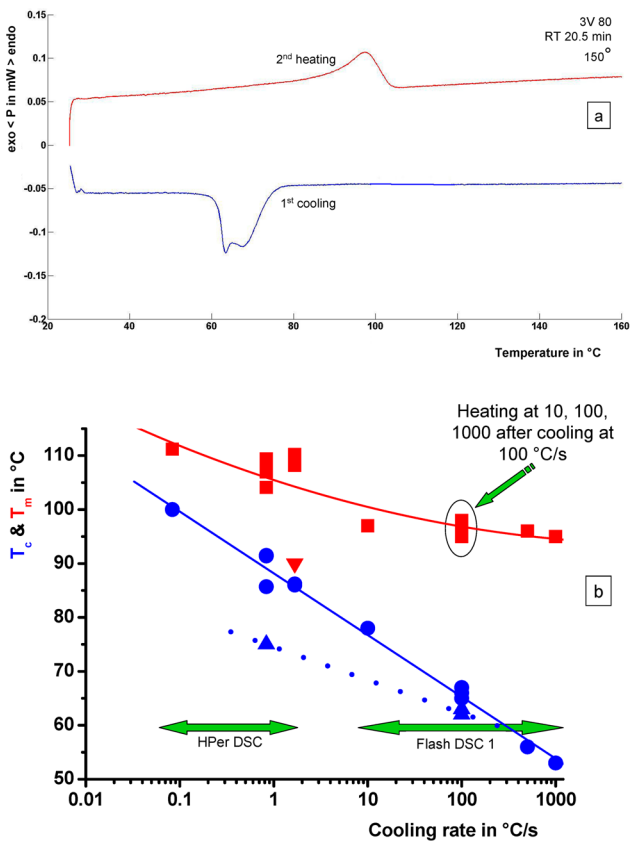


**Figure 7.** DSC measurements of sample TREF 3V 80. (a) An example of a flash DSC 1 measurement at 100 °C/s in both cooling and heating. (b) HPer DSC and flash DSC 1 results combined for the fractions in the molar mass range indicated in Figure 5 by the green box and by the black arrow, respectively. Peak maxima of $T_c$ and $T_m$ main and small peaks are represented by ●, ▲ and ■, ▼, respectively. The lines are guides to the eye.

results obtained by HPer DSC and by the flash DSC 1 are combined. The cooling data show a continuous decrease of $T_c$ with increasing cooling rate. The $T_m$ from the subsequent second heating measurements also shows a decrease. Both show continuity of the HPer DSC and flash DSC 1 data without any adjustment which is not trivial.[3,5] The small peak seen in Figure 6a, indicated by the blue triangle in Figure 5, has not been evaluated.

With respect to the behavior of $T_c$ as a function of cooling rate, analogous data are not found in literature up until now, and even so, sample results will differ with respect to branching content and distribution, molar mass, etc. A (very) limited comparison can be made with results on UHMWPE[5] for the onset temperature of crystallization as a function of cooling rate, varying from $10^{-3}$ to $10^4$ °C/s. For this tremendous variation over 7 decades, three different calorimeters (a Mettler-Toledo DSC 822, a PerkinElmer Pyris1 DSC, and a fast scanning calorimeter based on thin film chip sensors) have


dx.doi.org/10.1021/ma3008702 | Macromolecules 2012, 45, 5866−5880

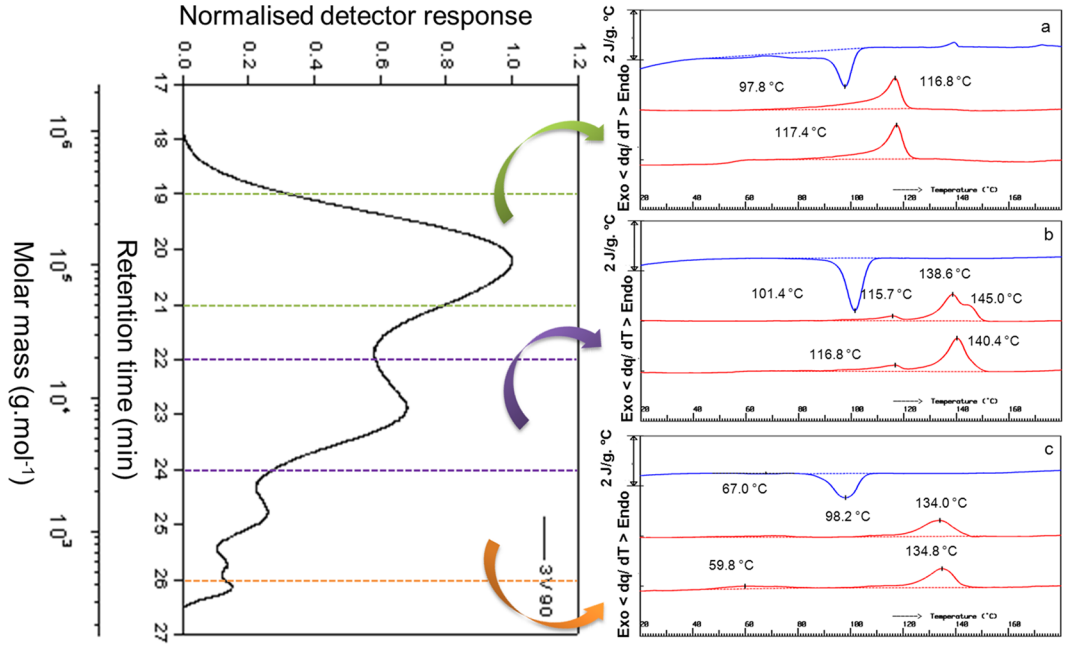


**Figure 8.** SEC-DSC analysis of sample TREF 3V 90. DSC curves for three representative samples of 3V 90.3, reflecting the coverage of the peaks in the SEC curve, see colored boxes; the high-*M* peak (sample 3V 90.3, 120°−160°); middle-*M* peak (3V 90.3, 180°−220°); and the two low-*M* peaks for sample 3V 90.3, 220°−260°).

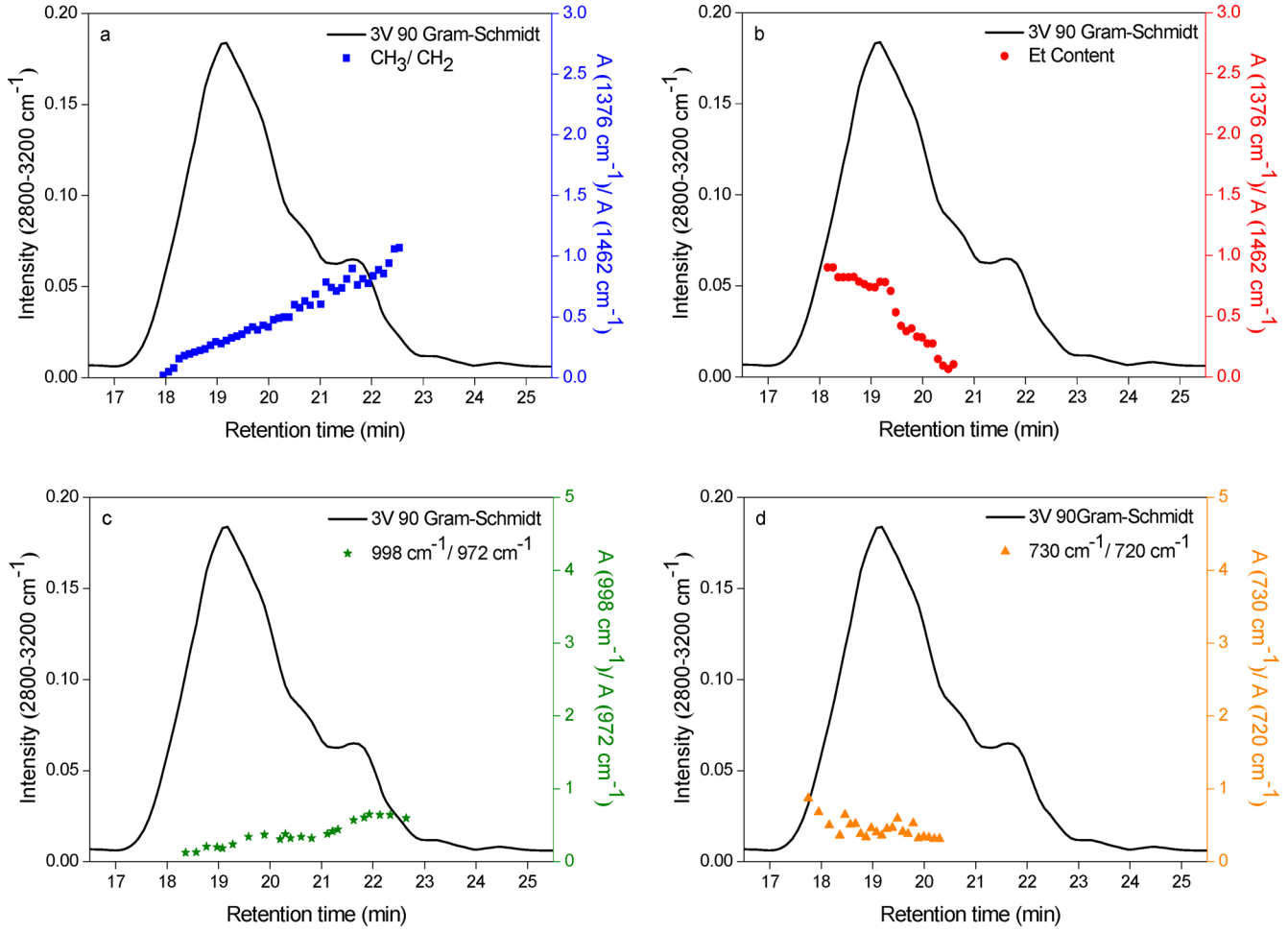


**Figure 9.** SEC-FTIR analysis of the 90 °C TREF fraction (3V 90) illustrating (a) the propylene ($CH_3/CH_2$) and (b) the ethylene (Et content) distributions as well as their crystallinity distributions (c) and (d), respectively.


dx.doi.org/10.1021/ma3008702 | *Macromolecules* 2012, 45, 5866−5880

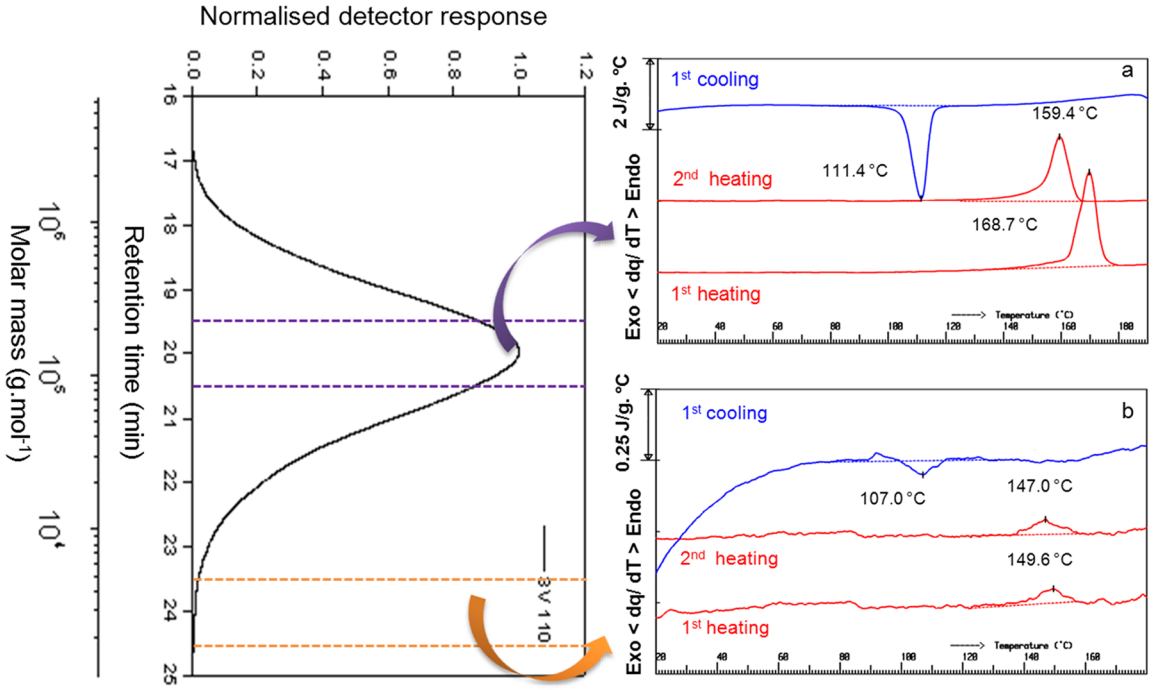


**Figure 10.** SEC-DSC analysis of sample TREF 3V 110. Measurements by HPer DSC on two SEC fractions, taken from the middle and very low-*M* part of the MMD as indicated in the graph on the left.

been used. Of interest is that these data show the same lowering of the crystallization peak maximum temperatures ($T_c$) with cooling rate ($\beta$)—the slope of $T_c(\beta)$—as found here, though at a 30 °C higher level.

The behavior of $T_m$ is interesting because it is seen to start to level off with increasing, preceding cooling rate. This occurs irrespective of the heating rate applied; see the $T_m$ data −98, 97, and 96 °C for heating at 10, 100, and 1000 °C/s, respectively, subsequent to cooling at 100 °C/s. In addition to the leveling off, a small variation of $T_m$ is typical for polymers which are able to reorganize very fast during heating, which is why one needs extremely high scan rates to hinder reorganization,[3,5,30] much higher than even the flash DSC 1 is capable of.

**Analysis of TREF Fraction 3V 90 (3.3 wt % of Total).** Besides the TREF fractions showing a bimodal-shaped SEC curve, one TREF fraction shows a multimodal SEC curve (see Figure 2). As can be seen in Figure 8, the MMD of 3V 90 comprises at least four well-distinguishable peaks. To find out what kind of polyolefins constitute these peaks, the DSC curves of three depositions have been measured, covering most of the MMD; see the three boxes indicating the parts of the MMD covered.

Following the same reasoning as for the other samples discussed, Figure 8a represents (see discussion at 3V 80) group 1 melting behavior: it shows the presence of a copolymerized polyethylene, more specifically low propylene content EPC, in the high-*M* part of the MMD for sample 3V 90, 120°−160°. The crystallization curve indicates the presence of more than one species crystallizing, though these do not show up separately in the melting curve.

The curves in Figure 8b (sample 3V 90, 180°−220°) representing the middle part of the MMD show group 3 behavior. The presence is seen of both PP having a lowered isotacticity or a "medium isotacticity" PP (a melting peak maximum of 138.6 °C) and in addition most probably a propylene-copolymerized PE, a low-propylene content EPC (a melting peak maximum at 115.7 °C). Again, it is seen that the crystallization temperatures of both the polymers present coincide, giving rise to a single crystallization peak with a maximum at 100.4 °C. The main melting peak at the highest temperatures shows two peaks at 138.6 and 145 °C, most probably caused by recrystallization. It illustrates that through a thermal history melting temperatures of 140 °C and higher can be realized; see also the first heating curve.

The third SEC fraction (sample 3V 90, 220°−260°) related to the low molar mass part of the MMD (see Figure 8c) represents group 2 melting behavior. Surprisingly, it again shows PP crystallinity, but at lower temperatures than the middle part of the MMD. This could be explained by the decreasing effect lower molar masses have on the crystallization and melting. Seeing the change in molecular structure with decreasing molar mass from the one extreme—high molar mass and low propylene content PE—to the other extreme—low molar mass and medium-isotacticity PP—it is evident that the middle molar mass fraction can be seen as an intermediate between the two extremes, showing the presence of both low propylene content EPC and medium-isotacticity PP.

According to FTIR (see Figure 9), in the highest-*M* part of the MMD—not covered by the boxes shown in Figure 8—propylene is present but not crystallized; thus only ethylene crystallinity will be present. In the high-*M* part of the MMD some PP crystallinity would be present, which is not confirmed by DSC. The middle-*M* part of the MMD indeed shows both ethylene and propylene crystallinity, while the low-*M* part of the MMD is characteristic of propylene crystallinity, ethylene crystallinity being absent.

**Analysis of TREF Fraction 3V 110 (18.8 wt % of Total).** According to Figure 1, this TREF fraction is the second largest fraction. The TREF fraction is the first one, which—with increasing TREF temperature—did show one melting endotherm on heating by DSC, while all TREF fractions eluting from 60 to 100 °C exhibited two melting endotherms.[8]


dx.doi.org/10.1021/ma3008702 | *Macromolecules* 2012, 45, 5866−5880

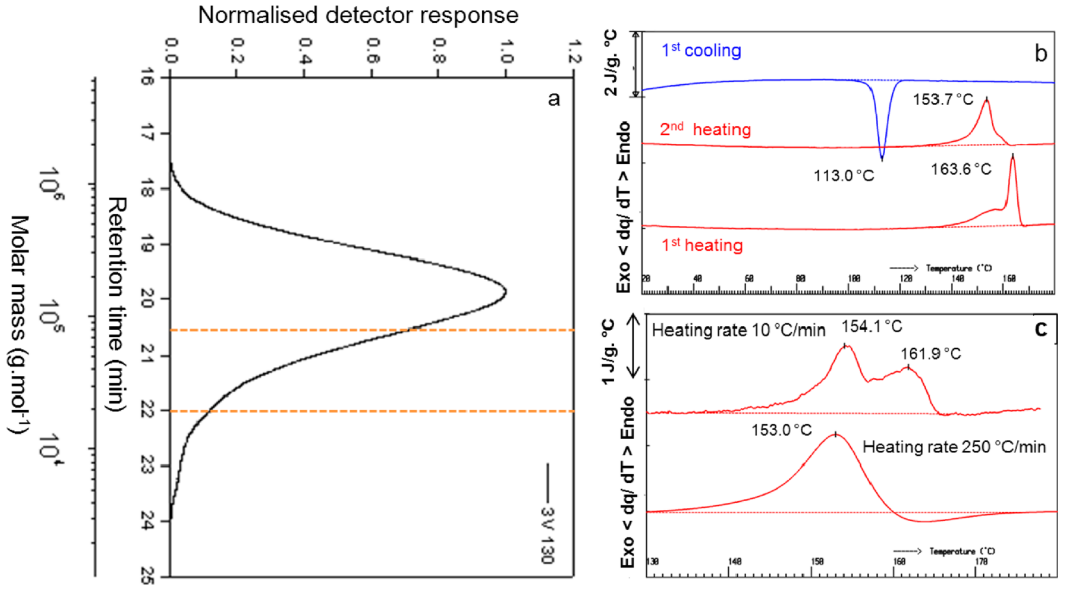


**Figure 11.** SEC-DSC analysis of sample TREF 3V 130. Crystallization and melting at 50 °C/min by HPer DSC of a low-*M* part of the SEC fraction of TREF fraction 3V 130; see box drawn on SEC curve on (a). Recrystallization is screened through variation of heating rate—10 and 250 °C/min in addition to 50 °C/min—subsequent to cooling at 50 °C/min.

Also, its SEC curve is unimodal (see Figure 10). For this fraction the DSC curve on the middle part of the MMD (see Figure 10a) clearly shows high-isotacticity PP with melting peak maximum temperatures of 158 (second heating curve) up to 168 °C (first heating). Crystallization still takes place around a low temperature, 111.4 °C, showing the high $\Delta T$ between the peak maximum temperatures of melting and crystallization, typical for PP. A very low molar mass fraction (see Figure 10b) still resembles a high-isotacticity PP (see the high crystallization temperature of 107 °C), though the melting peak maxima are lowered to 148 °C, probably mostly due to the decreasing effect of the low molar mass.

The DSC results are confirmed by the FTIR results, showing that the amount of propylene content is constant across the MMD as is the propylene crystallinity. No ethylene content is measurable, and no ethylene crystallinity is present. The DSC data also do not show the presence of polyethylene.

**Analysis of TREF Fraction 3V 130 (7.9 wt % of Total).** One fraction out of the total distribution is discussed, namely the SEC curve for the molar mass range covered by the orange box in Figure 11a. As seen in Figure 11b, this TREF fraction with the highest elution temperature of 130 °C shows crystallization (around the peak maximum of 113 °C) and melting of a high-isotacticity PP, with a melting main peak maximum at 153.7 °C and a shoulder at 160 °C for the second heating curve and 157 °C (shoulder) and 163.6 °C (main peak maximum) for the first heating curve.

The DSC data do not show the presence of polyethylene. Of interest is that—analogous to TREF fraction 3V 90—the shoulders and main peaks are most probably related to each other via recrystallization. To prove this, a variation of the heating rate subsequent to crystallization during cooling at 50 °C/min has been applied: besides heating at the same rate of 50 °C/min subsequent to cooling, heating at 10 and 250 °C/min have also been realized, presented in Figure 11c. Heating at 250 °C/min eliminates the highest melting peak maximum, by which the new maximum is situated at a slightly lowered value of 153 °C. Heating at 10 °C/min strengthens recrystallization, giving rise to two pronounced maxima. Clearly, the peak without recrystallization is marked by a maximum at ∼154 °C while (if melting−recrystallization−remelting occurs) a second, high-temperature peak arises at ∼162 °C at the expense of the low-temperature peak. Heating at 250 °C/min from 160 °C on results in an "overshoot": the experimental curve lies under the line extrapolated for the melt. However, this phenomenon does not influence the conclusions with respect to recrystallization.

**DSC Results on Melting of TREF-SEC Cross-Fractions: An Overview.** Hitherto, salient DSC curves of specific TREF-SEC cross-fractions have been presented. Figure 12 gives an overview by displaying melting peak maximum temperatures, measured at 50 °C/min, on SEC fractions for all TREF fractions studied. The cross-fractions have been divided into two groups on the basis of high or low $\Delta T$, meaning as before the difference between the peak maximum temperatures for melting, $T_m$, and crystallization, $T_c$ (not shown here), $\Delta T = T_m - T_c$. Propylene crystallinity relates to crystallization and melting behavior with a higher $\Delta T$ and (usually) a higher $T_m$ compared to ethylene-based polymers. From Figure 12b, a good correlation between $T_m$ and $T_{elution}^{TREF}$ is seen for both groups of cross fractions having propylene and ethylene crystallinities. The group with propylene crystallinity shows an increase of $T_m$ and $T_{elution}^{TREF}$ because of increasing isotacticity resulting in longer isotactic propylene sequences. The group with ethylene crystallinity shows an increase of $T_m$ and $T_{elution}^{TREF}$ because of decreasing propylene content, resulting in longer ethylene sequences within the chains of these ethylene−propylene copolymers (EPC). The lowest $T_m$ values are expected for ethylene−propylene rubbers (EPR) having short ethylene sequences. However, EPR, which is supposed to crystallize at (sub)ambient temperatures, and therefore it shows up in the TREF fraction 30 °C, will be reported separately. Overlap between the two groups of the melting temperatures is seen at the mid-elution temperatures. In the low-*M* range of the molar mass distribution no ethylene crystallinity is present; however, for higher molar masses both ethylene and propylene crystallinities are seen.


dx.doi.org/10.1021/ma3008702 | *Macromolecules* 2012, 45, 5866−5880

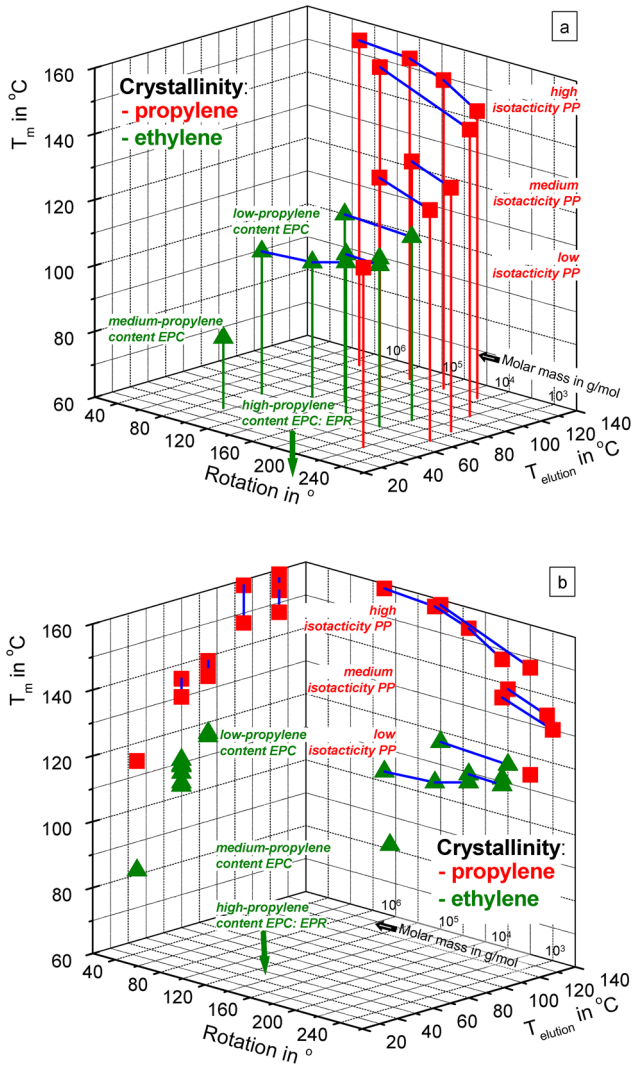


**Figure 12.** Correlation of melting temperature from DSC, molar mass (from SEC) and TREF fractionation for various samples TREF 3 V x. Melting related to ethylene and propylene crystallinities is represented by (▲) and (■), respectively. (a) 3D $T_m^{max}$ of SEC fractions—denoted by the average angle of rotation of the disk, see also the *M*-axis—of TREF fractions eluted at the average $T_{elution}$. (b) Two 2D projections of the data shown in (a) with the same axes.

**Linking Elution from TREF to Dissolution in DSC.** As was concluded at Figure 8 for 3V 90.3, the high molar mass fraction (rotation angle 120°−160°), see also Figure 13a, represents low-propylene content EPC. The medium molar mass fraction (rotation angle 180°−220°), see Figure 13b, was judged to be an intermediate between the extremes of PP and propylene copolymerized polyethylene(s) because it contains both components, though the PP content is much higher. The constituents of this intermediate fraction differ considerably with respect to their melting temperatures—116 °C for the PE component and 139 °C/145 °C for the PP component—while their crystallization maximum temperatures probably coincide at 100 °C (see Figure 8). Compared to PE types, PP can show an appreciable $\Delta T$. Despite these differences in the TREF dissolution procedure they both elute in between 80 and 90 °C, clearly pointing to the fact that $\Delta T$ is polymer- and solvent-dependent and different for crystallization and melting of the pure polymer (from and into the melt) and in solution. Thus, in the present case two different polymers, with different thermal behavior when measured from their melt state, elute in the same temperature range, masking these differences. Such occurrence of coeluting polymers with quite different molecular structures in the same temperature range leads to the complexity of interpreting the data and of elucidating the molecular structure.

To get an impression of the release of molecules during elution in a TREF setup, a dissolution experiment by DSC of 3V 90, in *p*-xylene, was performed. The concentrations are reasonably comparable: TREF 1 wt % and HPer DSC around 2 wt %. However, the cooling and heating rates are very different: very slow in case of TREF and 10−50 °C/min for DSC. Despite this, the result is clarifying (see Figure 13b): the final dissolution temperature by DSC of fraction 3V 90 coincides with the end temperature of the TREF range for the fraction used, 90 °C. Notice that the dissolution by DSC starts 25 °C before 80 °C which is caused by chains that partly dissolve, giving rise to a heat flow rate in the DSC and at the cost of a heat of fusion measured, but which cannot yet elute in TREF due to the presence of segments in the same chain that are more stable than the dissolved ones and by that still stay connected to other molecules within the same and/or other crystallites. In general, a chain will elute when the most stable segment of that chain dissolves. Because incorporation of ethylene and propylene units will always end up with ethylene and propylene distributions along the chains, various kinds of sequence lengths will be available.

Especially, for a given sequence of dissolved ethylene units or of isotactic propylene units, longer sequences and/or more perfect ones will in principle be still stable at the temperature of dissolution, and will dissolve and elute at higher temperatures and so on until the most stable sequence dissolves and the chain can elute. In contrast, the DSC will measure dissolution at the temperature/time of transition, whether they elute or not (yet).

From Figure 13a, one could conclude that in this case the dissolution range in TREF is beyond the 80−90 °C range. However, this "overshoot" is caused by recrystallization during heating of the solution in the DSC, giving a bimodal DSC heating curve with dissolution peak maxima at 83 and 95 °C. The fact that this sample has been eluted between 80 and 90 °C in TREF means that all material has been eluted for which the whole chain is dissolved before or at 90 °C and which chain is not capable anymore of recrystallization in xylene at 90 °C. If it would recrystallize just before and at 90 °C, then it would elute at temperatures higher than 90 °C, in the next elution temperature range of 90−100 °C.

To prove the occurrence of recrystallization, one usually increases the heating rate, by which less time is available for recrystallization and remelting. However, heating at 50 °C/min is a suitable but already a high heating rate for a polymer in solution in LVC pans. Therefore, the choice was made to decrease the cooling rate instead. Thus, the fact that recrystallization occurs for the SEC fraction 120°−160° of TREF fraction 3V 90.3 now follows from the experiment done (see Figure 13a) at 10 °C/min cooling and heating. At this slower rate the crystallization is better in terms of stability of the crystallites formed, by which the possibility of the occurrence of recrystallization is less. Indeed, the first, low-temperature melting peak is larger and the second, high-temperature remelting peak smaller. Decreasing the cooling rate further would remove the second high-temperature peak


dx.doi.org/10.1021/ma3008702 | *Macromolecules* 2012, 45, 5866−5880

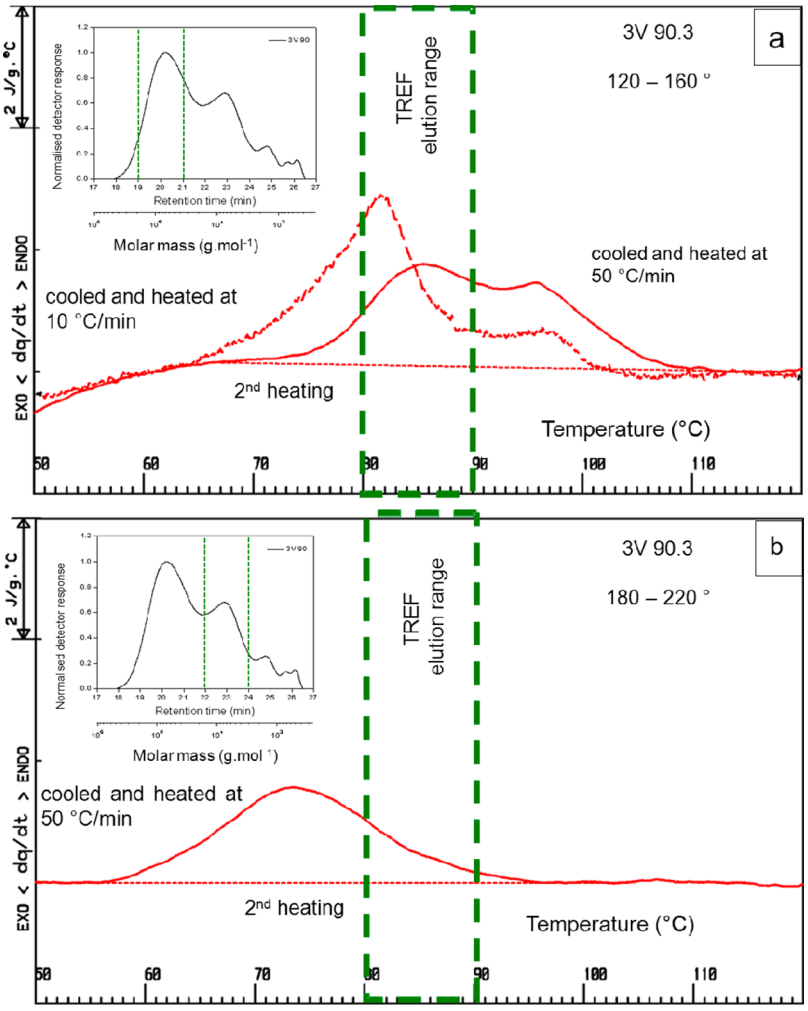


**Figure 13.** SEC-solution DSC analysis of sample TREF 3V 90. (a) Dissolution curves of 0.495 mg in approximately 20 mg of *p*-xylene at 10 and 50 °C/min subsequent to cooling at 10 (···) and 50 °C/min (−), respectively, of SEC fraction 120°−160° of TREF fraction 3V 90.3. (b) Dissolution curves of 0.345 mg in ∼20 mg of *p*-xylene at 50 °C/min subsequent to cooling at 50 °C/min (−) of SEC fraction 180°−220° of TREF fraction 3V 90.3. Both samples were measured between 10 and 130 °C with an isothermal stay of 15 min at 130 °C. The TREF elution temperature range of 80−90 °C is indicated by a green box. Insets: the parts of the MMD by SEC as covered by the samples are indicated by boxes as before.

fully leaving the low-temperature melting peak ending around 90 °C as expected from the TREF temperature range of 80−90 °C. Again, the dissolution starts earlier, ∼15 °C before 80 °C.

Having this in mind, the results found by HPer DSC are reasonable—even though it is operated at much higher scan rates compared to TREF experiments. Thus, from these preliminary experiments it is clear that measuring of crystallization and dissolution in liquids like *p*-xylene looks to be very rewarding: it opens possibilities to use HPer DSC as an extremely fast technique enabling designing of an optimal TREF elution temperatures scheme and the same for determination of optimal temperatures of crystallization in a liquid using CRYSTAF. Finally, to arrive at a useful method, it would be of interest to systematically study the occurrence of recrystallization as a function of molar mass and composition.

## 4. CONCLUSIONS

For the analysis of the complex molecular structure of impact PP various sophisticated techniques and methods have been combined. Starting with preparative TREF of the bulk IPC dissolved in xylene, various fractions were obtained at temperatures between 30 and 130 °C. Each fraction was subsequently fractionated by SEC and continuously deposited on a rotating disk wrapped with aluminum foil, under evaporation of the TCB using the LC transform interface. Fractions deposited in this way were measured by HPer DSC and compared with FTIR data. FTIR provided the ethylene and propylene content as a function of the rotating angle of the disk, which is related to the MMD. In addition, FTIR shows whether ethylene and/or propylene crystallinity had been developed, which was also presented as a function of MMD. For HPer DSC, samples of the TREF-SEC cross-fractions obtained were cut from the aluminum disk, resulting in 7 parts that vary in molar mass. Increasing the scan rates to 50 °C/min gave reasonable to good DSC curves, and in all cases the thermal behavior could be recorded very well. In the case that crystallization and melting occurred, it could be decided in most cases—e.g. on the basis of the difference between the peak maximum temperatures for melting ($T_m$) and crystallization ($T_c$)—what kind of polymer(s) caused the corresponding DSC peaks. Combining the findings with results from FTIR showed these to be complementary and unanimous and to be very useful in order to arrive at the complete picture of molecular structure.


dx.doi.org/10.1021/ma3008702 | *Macromolecules* 2012, 45, 5866−5880

The first fraction was eluted by TREF at 30 °C; however, this TREF fraction will be discussed in more detail in a separate study. The following TREF fractions, with eluting temperatures of 60 °C (3.4 wt %) and 80 °C (3.5 wt %), displayed bimodal SEC curves while the MMD of TREF fraction 90 °C (3.3 wt %) comprised at least four well-distinguishable SEC peaks. The higher TREF temperature fractions analyzed—110 °C (18.8 wt %, second largest) and 130 °C (7.9 wt %)—were unimodal. Together with TREF fraction 120 °C (47.8 wt %, largest), by their high weight percentage (in total almost 75 wt %), these fractions dominate in the characterization results and these often just seem to resemble bulk PP. Nevertheless, the smaller fractions can have a significant influence on properties, e.g., impact properties, far beyond from what one would expect on the basis of their weight percentage.

The samples for DSC were taken in such a way that information about the underlying molecular structure could be obtained. It turned out that in the lower *M* part of the MMD only propylene crystallinity was present. At intermediate and high *M*, both ethylene and propylene crystallinities were found to be related to polyethylene varying in propylene content and to polypropylene varying in isotacticity, respectively. With increasing TREF elution temperature the isotacticity of the polypropylene increased appreciably, leading to longer sequences of isotactic polypropylene and concomitant increasing melting temperatures. At the same time cross-fractions showing ethylene crystallinity were seen to be ethylene–propylene copolymers (EPC) with various ethylene and propylene sequence length distributions. With increasing TREF elution temperature their ethylene sequence lengths increased because of the decreasing amount of propylene incorporated in the chains.

As can be expected for the present components constituting the impact PP copolymer studied here, the DSC curves resemble metastable states with associated reorganization phenomena including recrystallization. Therefore, though the PerkinElmer DSC 8500 is quite capable to measure at 50 °C/min samples having such minute amounts of material as in the present case, to find out to what extent the scan rate is of importance it was varied by taking rates of 5, 50, 100, and 200 °C/min. For the same reason, measurements at 10, 100, and 1000 °C/s with the Mettler-Toledo flash DSC 1 have also been added. A first and important conclusion from these measurements is that continuity of the $T_c$ and $T_m$ data was found for the HPer DSC and the flash DSC 1. In this scan rate range spanning over 4 decades—from ∼0.1 to 1000 °C/s—$T_c$ dropped linearly in this restricted area, while the decrease of $T_m$ leveled off at the high scan rates, signifying that the melting process is dominated by fast reorganization processes: too fast for the present instrumentation to be influenced significantly.

Crystallization and dissolution measurements with the DSC 8500 on fractions in *p*-xylene gave useful information—after correction for recrystallization—on the lowering of $T_c$ and $T_m$ compared to crystallization and melting without liquid, from and into the melt state, even though the cooling and heating rates were much higher. This method is thought to be of interest for designing experiments using a solvent, like TREF and CRYSTAF, and in general fractionation by way of crystallization and dissolution in a solvent.

Finally, though the samples measured by HPer DSC were of the order of a few tens of micrograms, the limit has not been reached yet: it should be possible to work on sample masses down to the low microgram or high nanogram level. For even lower sample masses one can rely on the flash DSC 1.

The fact that the molecular properties can be correlated with thermal properties at very high heating and cooling rates promises to be the breakthrough for a better understanding of melting and crystallization under the conditions of materials processing, e.g., extrusion. This, in our opinion, is a significant advance in the present field of research.

## AUTHOR INFORMATION

### Notes

The authors declare no competing financial interest.

## REFERENCES


(1) Kaminsky, W. *Macromol. Chem. Phys.* **2008**, *209*, 459–466.
(2) Cheruthazhekatt, S.; Pijpers, T. F. J.; Harding, G. W.; Mathot, V. B. F.; Pasch, H. *Macromolecules* **2012**, *45*, 2025–2034.
(3) Schick, C. *Anal. Bioanal. Chem.* **2009**, *395*, 1589–1611.
(4) Zhuravlev, E.; Schick, C. *Thermochim. Acta* **2010**, *505*, 1–13.
(5) Zhuravlev, E.; Schick, C. *Thermochim. Acta* **2010**, *505*, 14–21.
(6) Pijpers, T. F. J.; Mathot, V. B. F.; Goderis, B.; Scherrenberg, R. L.; van der Vegte, E. W. *Macromolecules* **2002**, *35*, 3601–3613.
(7) Mathot, V. B. F.; Pyda, M.; Pijpers, T. F. J.; V Poel, G. V.; van de Kerkhof, E.; van Herwaarden, S.; van Herwaarden, F.; Leenaers, A. *Thermochim. Acta* **2011**, *522*, 36–45. See www.mt.com/TA-FlashDSC and www.scite.nl.
(8) de Goede, E.; Mallon, P.; Pasch, H. *Macromol. Mater. Eng.* **2010**, *295*, 366–373.
(9) Mirabella, F. M. *Polymer* **1993**, *34*, 1729–1735.
(10) Zhang, C.; Shangguan, Y.; Chen, R.; Wu, Y.; Chen, F.; Zheng, Q.; Hu, G. *Polymer* **2010**, *51*, 4969–4977.
(11) Mathot, V. B. F. The Crystallization and Melting Region. In *Calorimetry and Thermal Analysis of Polymers*; Hanser Publishers: Munich, 1994; Chapter 9, pp 231–299.
(12) Mandelkern, L. *Crystallization of Polymers*; Cambridge University Press: Cambridge, 2004; Vol. 2.
(13) Phuong-Nguyen, H.; Delmas, G. *Thermochim. Acta* **1994**, *238*, 257–275.
(14) Monrabal, B. *J. Appl. Polym. Sci.* **1994**, *52*, 491–499.
(15) Luruli, N.; Pijpers, T.; Brüll, R.; Grumel, V.; Pasch, H.; Mathot, V. *J. Polym. Sci., Part B: Polym. Phys.* **2007**, *45*, 2956–2965.
(16) Krumme, A.; Basiura, M.; Pijpers, T.; Poel, G. V.; Heinz, L. C.; Brüll, R.; Mathot, V. B. F. *Mater. Sci.* **2011**, *17*, 260–265.
(17) Holtrup, W. *Macromol. Chem.* **1977**, *178*, 2335.
(18) Mathot, V. Polycon "84 LLDPE" The Plastics and Rubber Institute London; proceedings 1 (1984).
(19) Mathot, V. B. F.; Pijpers, M. F. J. *Polym. Bull.* **1984**, *4*, 297–304.
(20) Macko, T.; Brüll, R.; Zhu, Y.; Wang, Y. *J. Sep. Sci.* **2010**, *33*, 3446–3454.
(21) Cong, R.; deGroot, W.; Parrott, Al.; Yau, W.; Hazlitt, L.; Brown, R.; Miller, M.; Zhou, Z. *Macromolecules* **2011**, *44*, 3062–3072.
(22) Ginzburg, A.; Macko, T.; Dolle, V.; Brüll, R. *Eur. Polym. J.* **2011**, *47*, 319–329.
(23) Shan, C. L. P.; Miller, M.; Lee, D.; Zhou, Z. *Macromol. Symp.* **2012**, *312*, 1–19.
(24) Eynde, S. V.; Mathot, V.; Koch, M. H. J.; Reynaers, H. *Polymer* **2000**, *41*, 3437–3453.
(25) Mathot, V. B. F.; Fabrie, C. C. M. *J. Polym. Sci., Part B: Polym. Phys.* **1990**, *28*, 2487–2507.
(26) Mathot, V. B. F.; Fabrie, C. C. M.; Tiemersma-Thoone, G. P. J. M.; Van Der Velden, G. P. M. *J. Polym. Sci., Part B: Polym. Phys.* **1990**, *28*, 2509–2526.
(27) Karssenberg, F. G.; Mathot, V. B. F.; Zwartkruis, T. J. G. *J. Polym. Sci., Part B: Polym. Phys.* **2006**, *44*, 722–737.
(28) Mathot, V. B. F.; Scherrenberg, R. L.; Pijpers, T. F. J. *Polymer* **1998**, *39*, 4541–4559.

(29) Poel, G. V.; Mathot, V. B. F. *Thermochim. Acta* **2007**, *461*, 107−121.
(30) Minakov, A. A.; van Herwaarden, A. W.; Wien, W.; Wurm, A.; Schick, C. *Thermochim. Acta* **2007**, *461*, 96−106.